

perpendicular to the electric dipole moment or little magnetic moment is induced by the stretching of the ligands in the ferric high-spin state and CO in the ferrous low-spin state. The relative orientation of the electric and magnetic dipole moments induced by the stretching of a ligand is approximately parallel for the cyanide but antiparallel for the azide in the ferric low-spin state. The orientation of the electric dipole moment depends on the coordination geometry of the ligand. Therefore, VCD is promising as to new insights into the electronic states as well as the coordination geometry of hemeoproteins. Further studies on the VCD enhancement mechanism of porphyrin ligands are currently in progress.

**Acknowledgment.** This work was supported in part by a grant from the Ministry of Education, Science, and Culture of Japan.

### High- $T_c$ Molecular-Based Magnets: A Ferromagnetic Bimetallic Chromium(III)–Nickel(II) Cyanide with $T_c = 90$ K

V. Gadet, T. Mallah, I. Castro,<sup>1</sup> and M. Verdaguer\*

Laboratoire de Chimie des Métaux de Transition  
URA CNRS 419, Université Pierre et Marie Curie  
4 Place Jussieu, 75252 Paris, France

P. Veillet

Institut d'Electronique Fondamentale  
URA CNRS 22, Université de Paris Sud  
91405 Orsay, France

Received June 15, 1992

$\text{CsNi}[\text{Cr}(\text{CN})_6] \cdot 2\text{H}_2\text{O}$  obtained by slow addition of a dilute aqueous solution of a  $\text{Ni}^{\text{II}}$  salt to a concentrated aqueous solution of freshly prepared  $\text{Cs}_2\text{K}[\text{Cr}(\text{CN})_6]$  (1/1 molar ratio) exhibits a spontaneous magnetization at  $T_c = 90$  K, due to a genuine short-range ferromagnetic exchange interaction. The elemental analysis fits with the proposed formula. The powder diffraction data display patterns of a face centered cubic cell with a unit cell parameter  $a = 10.57$  Å. X-ray absorption data show octahedral  $\text{Cr}^{\text{III}}$  and  $\text{Ni}^{\text{II}}$  ions surrounded respectively by six carbon atoms at 2.06 Å and six nitrogen atoms at 2.10 Å. The  $\text{Cr}(\text{CN})_6$  group appears unchanged in the solid. The heavy atom peak in the Fourier transform, at  $a/2$ , at both edges confirms the presence of a three-dimensional (3D) bimetallic network with  $\text{CN}^-$  as a bridging ligand.

In the last few years, different groups have obtained encouraging results in the field of molecular-based ferromagnets, either with organic (i.e., fullerene),<sup>2</sup> metal–organic,<sup>3,4a</sup> metal–radical,<sup>4b</sup> or bimetallic<sup>4c</sup> systems. Among the data with an available crystal structure, the true molecular systems present the lowest  $T_c$ . One way to enhance the  $T_c$  value is to deal with bimetallic one-dimensional (1D) systems,<sup>4b,c</sup> with a strong and controlled interaction along one direction. However, the problem of inducing 1D–3D crossover in order to obtain the wanted magnets remains. Our approach is to build directly 3D frameworks through mild chemistry methods using molecular precursors specially chosen to achieve a 3D covalent bonding network between spin-bearing species. One of the simplest and most convenient molecular

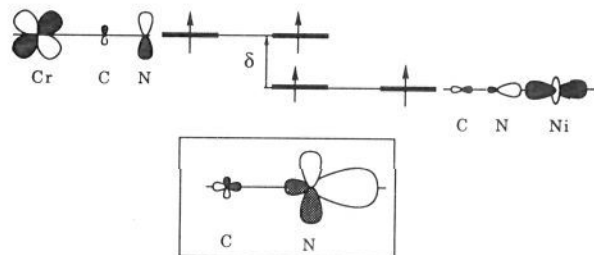


**Figure 1.** Orthogonality between  $t_{2g}(xy)$   $\text{Cr}^{\text{III}}$  and  $e_g(z^2)$   $\text{Ni}^{\text{II}}$  magnetic orbitals in  $\text{Cs}^{\text{I}}\text{Ni}^{\text{II}}[\text{Cr}^{\text{III}}(\text{CN})_6] \cdot 2\text{H}_2\text{O}$ .

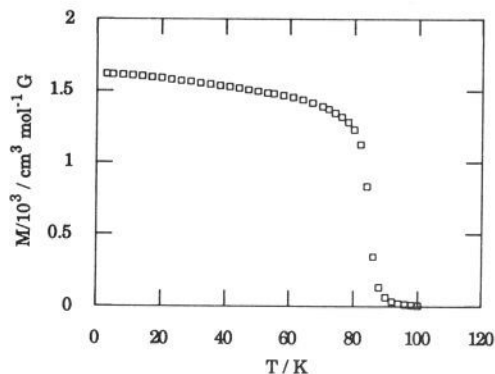


**Figure 2.** Field cooled magnetization curve  $M = f(T)$  at  $H = 10$  G.

building blocks can be found in the hexacyanometalate family  $[\text{B}(\text{CN})_6]^{n-}$ .

The old but evergreen family of Prussian blue like bimetallic complexes leads to various  $k/l$  stoichiometries,  $\text{A}_k[\text{B}(\text{CN})_6]_l \cdot m\text{H}_2\text{O}$ .<sup>5</sup> When  $k/l > 1$ , the structure presents  $\text{B}(\text{CN})_6$  vacancies and high water content. Ten years ago, among a series of uncoupled paramagnetic systems, Babel et al.<sup>6</sup> reported on the ferrimagnetic system  $\text{Cs}^{\text{I}}\text{Mn}^{\text{II}}[\text{Cr}^{\text{III}}(\text{CN})_6] \cdot \text{H}_2\text{O}$ , with  $T_c$  value = 90 K. Using  $[\text{Fe}^{\text{III}}(\text{CN})_6]^{3-}$  ( $d^5$ ,  $(t_{2g})^5$ , low-spin  $S = 1/2$ ) as a precursor, we obtained ferrimagnetic (with  $\text{A}^{\text{II}} = \text{Mn}^{\text{II}}$  and  $\text{Co}^{\text{II}}$ ) and ferromagnetic (with  $\text{A}^{\text{II}} = \text{Cu}^{\text{II}}$  and  $\text{Ni}^{\text{II}}$ ) systems and a  $k/l = 3/2$  stoichiometry, with  $T_c$  ranging from 9 to 23 K.<sup>7</sup> However, using chromicyanide instead of ferricyanide, we obtain a spectacular enhancement of  $T_c$ <sup>8</sup> (in the 55–65 K range), still with the  $3/2$  stoichiometry. The presence of  $\text{B}(\text{CN})_6$  vacancies probably hinders a full interaction through the whole compound. To avoid such vacancies, a cesium cation  $\text{Cs}^{\text{I}}$  was used to stabilize  $1/1$  stoichiometric compounds. We report here the magnetic properties of  $\text{Cs}^{\text{I}}\text{Ni}^{\text{II}}[\text{Cr}^{\text{III}}(\text{CN})_6] \cdot 2\text{H}_2\text{O}$ , which orders ferromagnetically at 90 K.

The susceptibility and magnetization measurements were performed using a SQUID magnetometer. Upon cooling down from room temperature to 90 K,  $\chi_M T$  increases continuously, expressing a short-range ferromagnetic exchange interaction between nearest metallic ions. Such a short-range interaction, expected from the strict orthogonality of the  $t_{2g}$  orbitals of  $\text{Cr}^{\text{III}}$  and the  $e_g$  orbitals of  $\text{Ni}^{\text{II}}$  (Figure 1), had already been predicted by Ginsberg<sup>9</sup> and experimentally demonstrated by Pei et al.<sup>10</sup> At 90 K,  $\chi_M T$  diverges, suggesting a long-range ferromagnetic order. The field-cooled magnetization vs temperature plot at  $H = 10$  G in the 3–100 K range (Figure 2) presents a break at  $T_c = 90$  K confirming the onset of a 3D long-range ferromagnetic order within the compound. The value is well above that observed for the  $3/2\text{Ni}_3[\text{Cr}(\text{CN})_6]_2 \cdot 12\text{H}_2\text{O}$  compound ( $T_c = 60$  K),<sup>8</sup> showing the importance of a lack of  $[\text{Cr}(\text{CN})_6]^{3-}$  vacancies in these com-

(1) Permanent address: Departament de Química Inorgànica, Facultat de Química, Dr Moliner 50, Burjassot, Valencia, Spain.

(2) Allemand, P. M.; Khemani, K. C.; Koch, A.; Wudl, F.; Holczer, K.; Donovan, S.; Grüner, G.; Thompson, J. D. *Science* 1991, 253, 301.

(3) Manriquez, J. M.; Yee, G. T.; McLean, R. S.; Epstein, A. J.; Miller, J. S. *Science* 1991, 252, 1415.

(4) *Molecular magnetic materials*; Gatteschi, D., Kahn, O., Miller, J. S., Palacio, F., Eds.; NATO ASI Series, Series E, Vol. 198; Kluwer: Dordrecht, 1991; (a) Miller, J. S., pp 151–158; (b) Rey, P., pp 203–214; Caneschi, A., pp 215–232; (c) Kahn, O., pp 35–52.

(5) Lüdi, A.; Güdel, H. *Struct. Bonding (Berlin)* 1973, 14, 1.

(6) Griebler, W. D.; Babel, D. *Z. Naturforsch.* 1982, 87b, 832.

(7) Gadet, V., et al., pp 281–296 in ref 4.

(8) Gadet, V.; Mallah, T.; Verdaguer, M. Work in progress.

(9) Ginsberg, A. P. *Inorg. Chim. Acta, Rev.* 1971, 5, 45.

(10) Pei, Y.; Journaux, Y.; Kahn, O. *Inorg. Chem.* 1989, 28, 100.

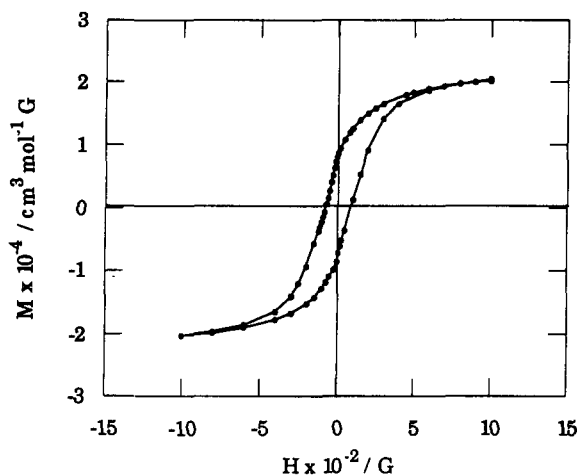


Figure 3. Hysteresis loop  $M = f(H)$  at 3 K.

pounds. The magnetization vs field curve of our sample at 3 K shows a hysteresis loop with a coercive field  $H_C = 71$  G and a remnant magnetization  $M_R$  of  $7.6 \times 10^3 \text{ cm}^3 \text{ mol}^{-1} \text{ G}$  (Figure 3).<sup>11</sup> The magnetization at high field ( $H = 4000$  G) corresponds to the expected value for parallel spins  $S_{\text{Ni}} = 1$  and  $S_{\text{Cr}} = 3/2$ .

All these features are consistent with the behavior of a ferromagnet synthesized from molecules (i.e., molecular-based). The value of  $T_C$  is sensitive to the stoichiometry, correlated to the water content.<sup>12</sup> Neutron diffraction, X-ray absorption experiments, and chemical conditioning of the compound, with fewer or no water molecules, are in progress to elucidate the effect of water molecules upon  $T_C$ .

(11) The  $H_C$  and  $M_R$  values are not an intrinsic property of the material, since they depend upon (i) the value when the applied field is reversed (here,  $H = 1000$  G) and (ii) the grain size of the sample. Increasing the grain size is underway.

(12) From our own experience and from a private communication from Prof. D. Babel.

### Valence Contrast by Synchrotron Resonance Scattering: Application to a Mixed-Valence Manganese Compound

Y. Gao, A. Frost-Jensen,<sup>†</sup> M. R. Pressprich, and P. Coppens\*

Chemistry Department  
State University of New York at Buffalo  
Buffalo, New York 14214

A. Marquez and M. Dupuis

IBM Corporation, Data Systems Division  
Department 48B/MS 428, Kingston, New York 12401

Received July 15, 1992

The tunability of synchrotron radiation makes it possible to vary the scattering power of atoms of specific elements in the vicinity of the atomic absorption edges. The effect is due to the contribution of low-lying electronically excited states to the X-ray scattering process, which is accounted for in the second Born approximation of X-ray scattering theory. The variation of the anomalous components of the atomic scattering,  $f'$  and  $f''$ , may be used to create a contrast between multiwavelength results that can be applied in the determination of atomic site occupancy.<sup>1</sup> In addition, the variation shows a chemical shift which is about 2.5 eV for each increase in unit of formal valency of vanadium,<sup>2</sup>

\* Author to whom correspondence should be addressed.

<sup>†</sup> Current address: Aarhus University, DK8000 Aarhus, C, Denmark.

(1) Coppens, P.; Lee, P.; Gao, Y.; Sheu, H.-S. *J. Phys. Chem. Solids* **1991**, *52*, 1267-1272.

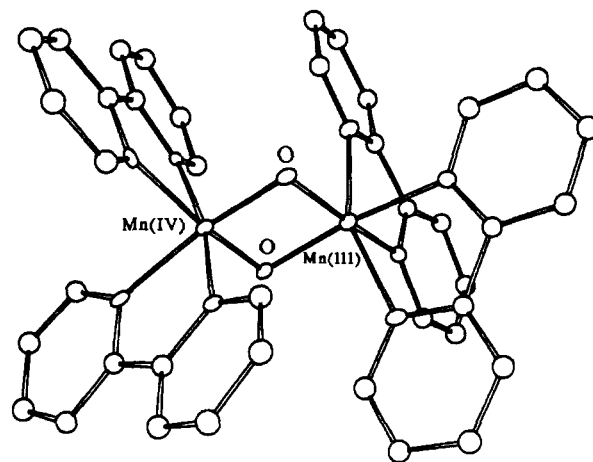


Figure 1. Diagram of the cation.

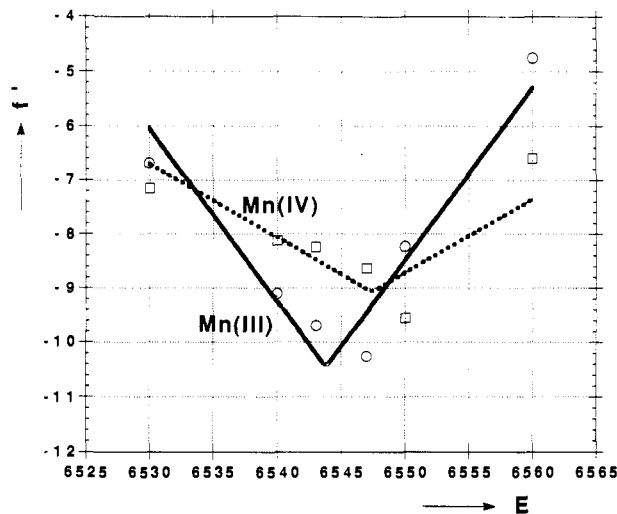


Figure 2. Triangle fit to  $f'$  values: solid line, Mn(III); broken line, Mn(IV).

and about 5 eV for Fe in  $\text{Fe}^{\text{II}}(\text{NH}_4)_2(\text{SO}_4)_2 \cdot 6\text{H}_2\text{O}$  relative to  $\text{Fe}^{\text{III}}(\text{NO}_3)_3$ .<sup>3</sup> This difference can be used to obtain direct information on the electronic environment of specific atoms, as shown in powder diffraction studies of mixed-valence solids by Attfield<sup>4</sup> ( $\text{Eu}_3\text{O}_4$ ), by Wilkinson, Cheetham, and Cox<sup>5</sup> ( $\text{GaCl}_2$ ), and in our work on  $\text{NbSe}_3$ .<sup>6</sup> We report here on a first application to a mixed-valence molecular crystal, in which  $f'$  is determined from the refinement of a set of selected reflection data collected at eight wavelengths on both sides of the absorption edge.

The enzyme-photosystem model compound  $(\mu\text{-dioxo})\text{Mn}(\text{2,2}'\text{-bipyridyl})_2(\text{BF}_4)_3 \cdot 3\text{H}_2\text{O}$  (Figure 1) was synthesized as described elsewhere.<sup>7</sup> It is centrosymmetric and isomorphous to the previously reported perchlorate salt.<sup>8</sup> A nearly cube-shaped crystal of volume  $0.0135 \text{ mm}^3$  was used for data collection at the SUNY X3 beamline at Brookhaven National Laboratory.

The intensities of a selected set of 24 reflections were collected at eight different energies around the Mn K edge at 6540 eV, using a Si(111) double-crystal monochromator. Structure factors obtained after absorption correction were refined in terms of the

(2) Wong, J.; Lytle, F. W.; Mesmer, R. P.; Maylotte, D. H. *Phys. Rev.* **1984**, *B30*, 5596.

(3) Coppens, P. *Synchrotron Radiation Crystallography*; Academic Press: London, 1992; p 125.

(4) Attfield, J. P. *Nature* **1990**, *343*, 46.

(5) Wilkinson, A. P.; Cheetham, A. K.; Cox, D. E. *Acta Crystallogr.* **1991**, *B47*, 155.

(6) Gao, Y.; Darovsky, A.; Pressprich, M. R.; Coppens, P. Site Specific Anomalous Scattering Study of the Valence Difference between the Nb Atoms in  $\text{NbSe}_3$ . 1992 NSLS User Meeting.

(7) Cooper, S. R.; Calvin, M. J. *Am. Chem. Soc.* **1977**, *99*, 6623-6630.

(8) Plaksin, P. M.; Stouffer, R. C.; Mathew, M.; Palenik, G. J. *J. Am. Chem. Soc.* **1972**, *94*, 2121-2122.